

Ivan Vitev

# Theoretical aspects of the EIC heavy flavor program

Joint EFo7 and EFo6 discussion: Heavy Flavor  
Physics at the EIC  
*October 2020*



# Letter of Interest

H. Abdolmaleki (IPM), M. Arratia (UC Riverside), Y.-T. Chien (SUNY Stony Brook), X. Dong (LBNL), M. Durham (LANL), Y. Furletova (JLab), M. Garzelli (Hamburg U.), V.P. Goncalves (UFPel), T. Hobbs (SMU), J. Huang (BNL), Y. Ji (USTC/LBNL), Z. Kang (UCLA), M. Kelsey (LBNL), X. Li (LANL), H.-W. Lin (MSU), M. Liu (LANL), S. Moch (Hamburg U.), P. Nadolsky (SMU), V. Okorokov (NRNU MEPhI), F. Olness (SMU), M. Ploskon (LBNL), S. Radhakrishnan (KSU/LBNL), J. Rojo (Nikhef), I. Schienbien (LPSC), S. Sekula (SMU), D. Shao (UCLA), E. Sichtermann (LBNL), G. Silveira (UFRGS & UERJ), G. Sterman (SUNY Stony Brook), I. Vitev (LANL), K. Xie (SMU), W. Xie (Purdue U.), Z. Ye (UIC)

30+ signators

## Letter of Interest: Heavy Flavors at the EIC

H. Abdolmaleki (IPM), M. Arratia (UC Riverside), Y.-T. Chien (SUNY Stony Brook), X. Dong (LBNL), M. Durham (LANL), Y. Furletova (JLab), M. Garzelli (Hamburg U.), V.P. Goncalves (UFPel), T. Hobbs (SMU), J. Huang (BNL), Y. Ji (USTC/LBNL), Z. Kang (UCLA), M. Kelsey (LBNL), X. Li (LANL), H.-W. Lin (MSU), M. Liu (LANL), S. Moch (Hamburg U.), P. Nadolsky (SMU), V. Okorokov (NRNU MEPhI), F. Olness (SMU), M. Ploskon (LBNL), S. Radhakrishnan (KSU/LBNL), J. Rojo (Nikhef), I. Schienbien (LPSC), S. Sekula (SMU), D. Shao (UCLA), E. Sichtermann (LBNL), G. Silveira (UFRGS & UERJ), G. Sterman (SUNY Stony Brook), I. Vitev (LANL), K. Xie (SMU), W. Xie (Purdue U.), Z. Ye (UIC)

The Electron-Ion Collider (EIC) Heavy Flavor Group is writing to express its interests in the future of high energy physics and the Snowmass 2021 planning process. We recognize the deep intellectual connections between particle and nuclear science and the rich collaborative opportunities that the EIC will bring in theory, computation, experiment, and detector technology [1]. We advocate for the inclusion of EIC science in the recommendations for the future of high energy physics in the US. Our primary interests align with the Energy Frontier of Snowmass 2021, with strong overlaps with the Theory and Computing Frontiers [2].

Open and hidden heavy-flavor production in deep-inelastic scattering needs a status review of the tools/theory to make precise predictions in the future EIC experiments. As heavy quarks introduce a new mass scale, the impact of flavor number schemes - fixed-flavor number (FFN) scheme and variable-flavor-number (VFN) scheme - on charm and bottom distributions has to be better understood [3,4].

Via neutral-current (NC) exchange in  $e+p/A$  collisions at the EIC, heavy flavor production can be used to probe the initial gluon distributions inside nucleon and nucleus. This can be used to constrain the gluon (nuclear) PDF especially in the large  $x_B$  region [5]. In the charged-current (CC) interaction channel with the scattered neutrino, heavy flavor and heavy flavor jet production offer the sensitivity to the strange quark sea [6]. The interpretation of data from these experiments may be complicated by a subtle interplay of effects arising from nuclear, target-mass, and other power-suppressed corrections, as well as potential contamination from target fragmentation. This requires a significance development in theory predictions and tools in order to extract valuable info (e.g. gluon and sea quark PDFs) from future data. One critical issue to be addressed is how to distinguish nPDF effects from other CNM effects through the analysis of future EIC data together with the data on heavy-flavor production at HERA and the LHC [7].

Many ambiguities remain regarding the possible role of heavy quarks - particularly charm - in hadronic and nuclear structure. A prime example of this is the issue of the nonperturbative or intrinsic charm contribution to the proton wave function [8,9]. Up-to-date, there is nearly a complete lack of measurements with direct sensitivity to nonperturbative charm in the nucleon. The ideal measurement would involve charm structure-function data in the high  $x > 0.1$  and intermediate  $Q \sim 10$  GeV region, which the EIC will be poised to extract with considerable precision. Similarly, the EIC will be well-positioned to not only constrain/isolate the presence of intrinsic charm but also to potentially determine its detailed origins in QCD. The EIC could shed light on this subject through a detailed exploration of the scale dependence of the nucleon's charm component. More broadly, there is a possible role to be played by charm-jet production in this area as well.

# Effect of flavor schemes on PDF extraction

## Follows discussion from

S. Alekhin et al. (2020)

- Different schemes and different prescriptions in the variable flavor number scheme
- Critical assessment and comparisons will be useful for the EIC

Fixed flavor schemes – typically at low virtualities

Variable flavor schemes – as one goes to higher energies, effectively resums

$$Q^2/m^2_c \text{ (or } Q^2/m^2_b)$$

### ABM

The ABMP16 PDF fit [5] is based on the FFN scheme in a part concerning heavy-flavor DIS production. Nonetheless, for the collider data on  $t$ -quark,  $W$ - and  $Z$ -boson production, where the VFN scheme is more relevant, the 5-flavor PDFs are constructed from the 3-flavor ones, see Eqs. (2)–(4), using currently available information on the heavy-quark OMEs and employing NNLO evolution for the matched PDFs. All relevant formulae are implemented in the code OPENQCDRAD (version 2.1), which is publicly available [43].

### CT

CT18 [7] uses the ACOT VFN scheme [26–28], specifically an NNLO realization [44] of the so-called S-ACOT- $\chi$  variant. The S-ACOT- $\chi$  VFN scheme features a slow rescaling of the parton momentum fractions  $z$  in the argument of the respective massless Wilson coefficient functions in  $F_{2,h}^{ZMVFN}$  in Eq. (12) by replacing  $z \rightarrow \chi = z \left(1 + \frac{4m_h^2}{Q^2}\right)$ , and restricting the integration range of  $z$  in the convolutions to  $x \left(1 + \frac{4m_h^2}{Q^2}\right) \leq z \leq 1$  with the Bjorken variable  $x$ . The slow rescaling is motivated by its properties to model energy conservation in the DIS production of heavy final states. Ref. [44] also explores a wider family of rescaling choices, which interpolate smoothly between  $z$  and  $\chi$ .

### MSTW

MMHT14 [8] uses the RT VFN scheme [30], specifically the TR' prescription from Ref. [45] for PDF fits at NNLO. The RT scheme requires as a constraint the continuity of physical observables in the threshold region, i.e., for the expression for  $F_{2,h}^{FFN}$  in Eq. (13) below and  $F_{2,h}^{ZMVFN}$  in Eqs. (12) above threshold. To that end, the derivative of the structure function,  $dF_2/d\ln Q^2$  is supposed to be continuous at the matching point  $Q^2 = m_h^2$  in the gluon sector. To achieve this modeling constraint, a  $Q^2$ -independent term is added above the matching point to the expression for  $F_{2,h}^{ZMVFN}$  to maintain continuity of the structure function. The TR' prescription specifies this procedure up to NNLO [45].

### NNPDF

NNPDF3.1 [9] uses the FONLL VFN scheme [29], which has been devised to combine the heavy-quark DIS structure functions and the ZMVFN expressions in analogy to Eq. (15). FONLL suppresses the difference of  $F_{2,h}^{ZMVFN}$  in Eq. (12) and the necessary subtraction term, i.e., the expression analogous to  $F_{2,h}^{asy}$  in Eq. (14), which is needed to avoid double counting, with a kinematical damping factor  $\left(1 - \frac{Q^2}{m^2}\right)^2$ . In this manner, it is guaranteed, that only  $F_{2,h}^{FFN}$  of Eq. (13) remains for virtualities  $Q^2 \simeq m_h^2$  near threshold. The variant FONLL-C is used to determine the PDFs at NNLO [29].

# BMSN prescription for VFNS, confronting HERA data

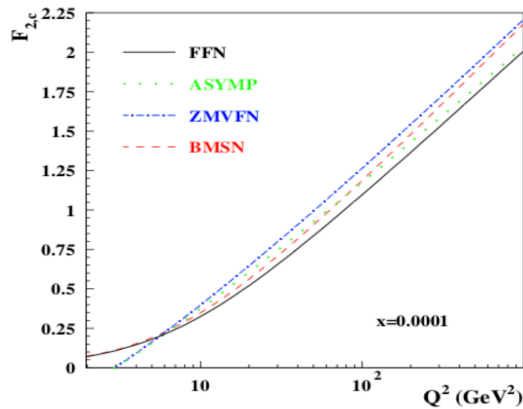
Realistic evaluations combine FFNS and VFNS, subtraction of double counting is required

$$F_{2,h}^{FFN} = \sum_{k=1}^{\infty} a_s^k(n_f) \sum_{i=q,g} H_{2,i}^{(k)}(n_f) \otimes f_i(n_f),$$

$$F_{2,h}^{ZMVFN} = \sum_{k=0}^{\infty} a_s^k(n_f+1) \sum_{i=q,g,h} C_{2,i}^{(k)}(n_f+1) \otimes f_i(n_f+1)$$

$$F_{2,h}^{asy} = \sum_{k=1}^{\infty} a_s^k(n_f) \sum_{i=q,g} H_{2,i}^{(k),asy}(n_f) \otimes f_i(n_f),$$

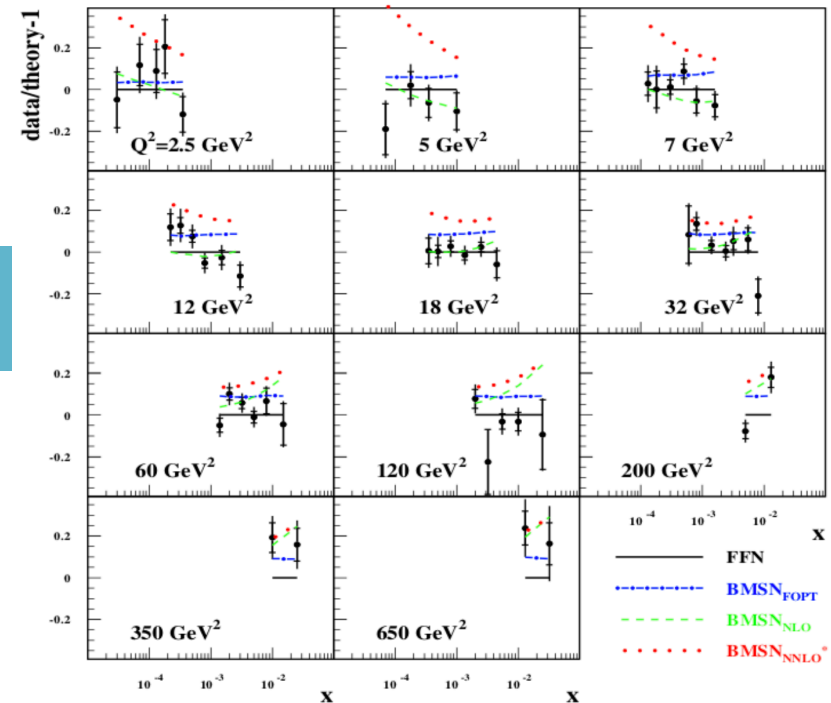
$$F_{2,h}^{BMSN} = F_{2,h}^{FFN} + F_{2,h}^{ZMVFN} - F_{2,h}^{asy}$$



S. Alekhin et al. (2020)

- Transitions between FFN and VFS
- Depending on order/prescription,  $Q^2$  – good description of DIS data

$\sigma_{red}^{cc}$  (HERA RunI+II combined)



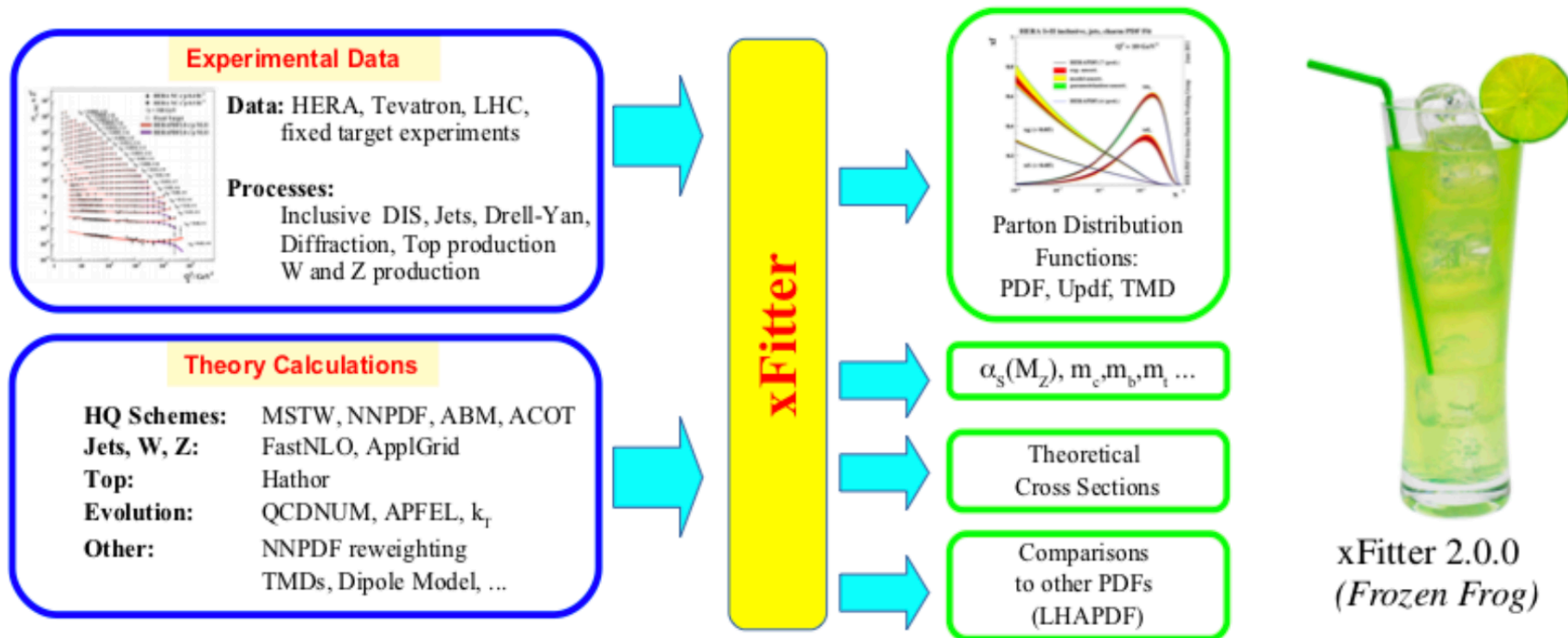
Confronting HF schemes with HERA data

# xFitter Team

V. Bertone et al. (2019)

Emphasizes the need for flexible tools for PDF analysis

- Can take input from various processes, notably DIS; can produce not only PDFs but also related alphas values, heavy quark masses



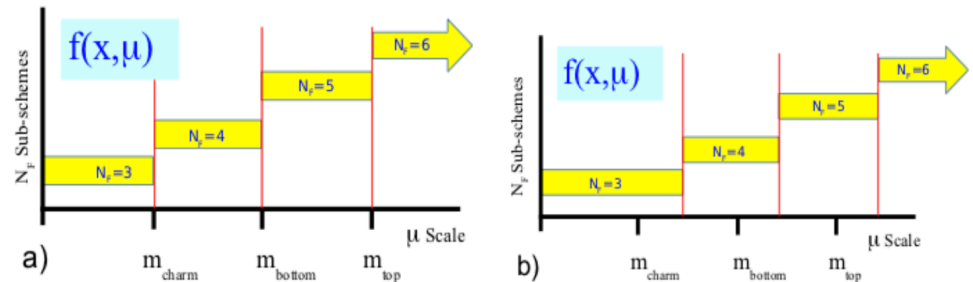
# xFitter Team Example - VFNs matching scales

A. Kusina et al. (2013)

## Hybrid variable flavor number scheme

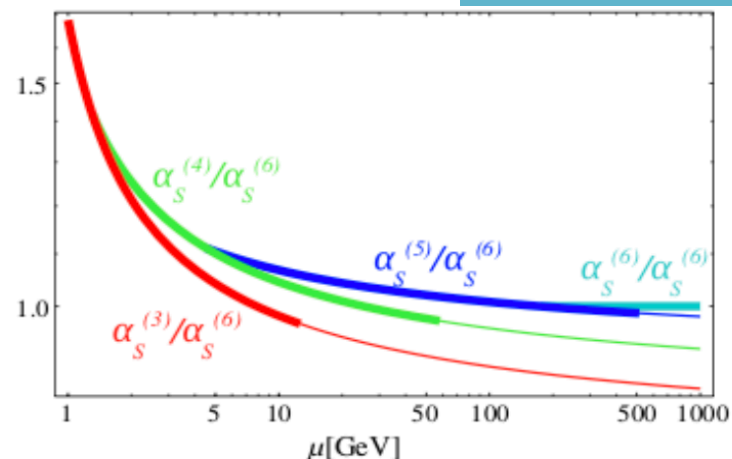
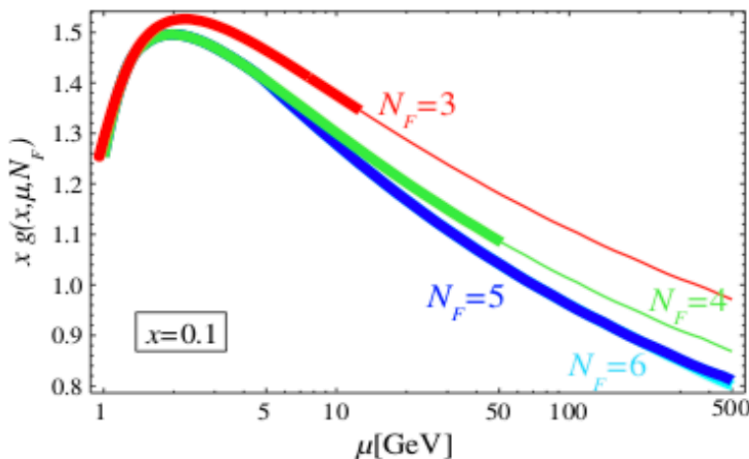
- Different choices of matching mass values. It allows the user, for example to use  $N_f=4$  above  $M_b$  scale for example

- (1) The PDFs and strong couplings with different  $N_F$  flavors coexist simultaneously.
- (2) The PDFs and strong couplings with one  $N_F$  value have a precise analytic relation to those with a different  $N_F$  value which is specified by the appropriate evolution equations and the  $\overline{MS}$  boundary conditions at  $\mu = m_{c,b,t}$  (cf., the Appendix).



In going to higher precision the differences from separation scales choice disappear

V. Bertone et al. (2018)

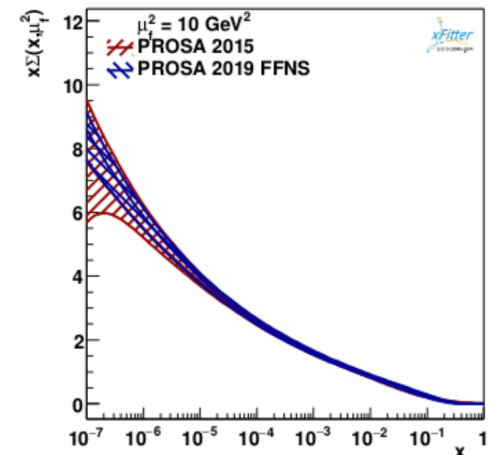
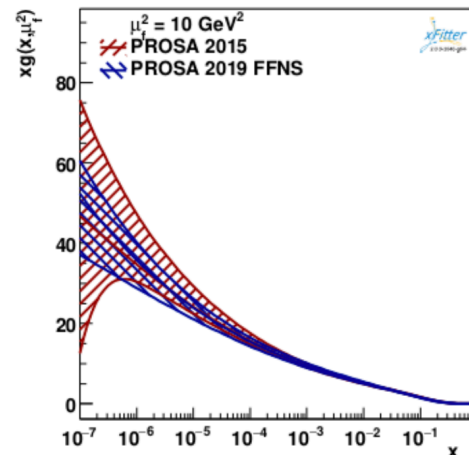
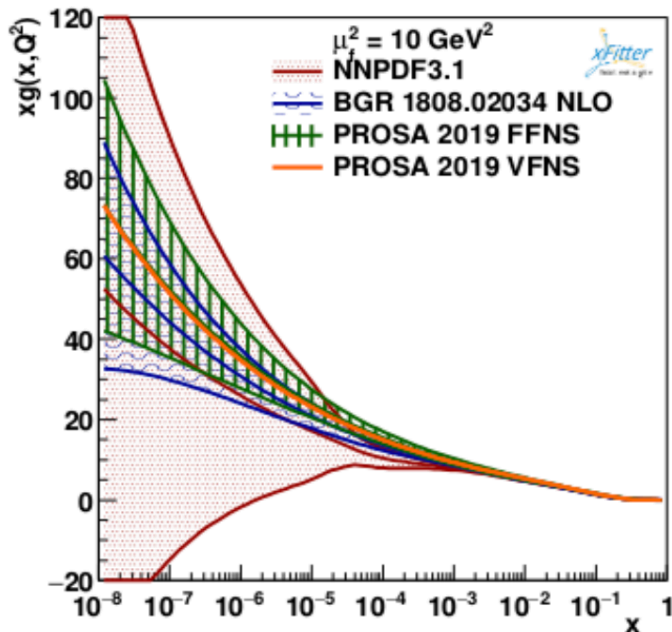


# Use of LHC data to constrain heavy flavor PDFs – PROSA collaboration

O. Zenaiev et al. (2018)

- Adding LHCb and ALICE data to the heavy flavor data from HERA

Inclusion of heavy flavor reduces PDF uncertainties for sea quarks and gluons at small  $x$ , especially FFNS



Important to do combined analysis at the EIC

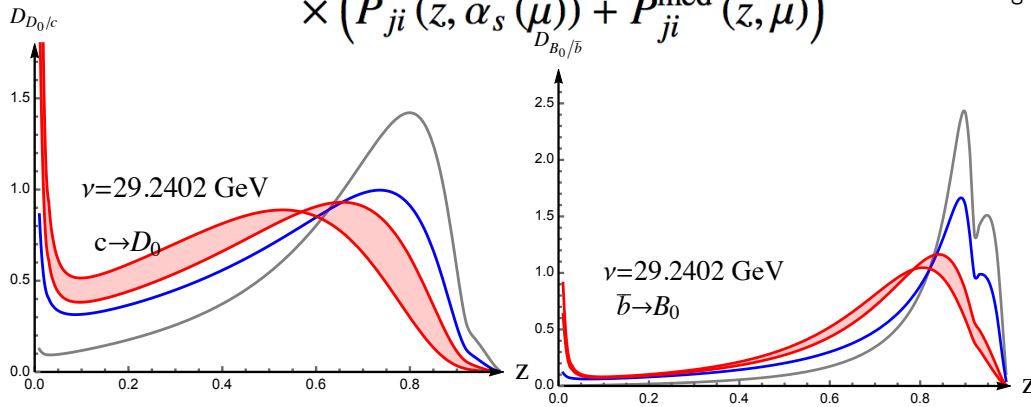
# Heavy meson production in e+p at EIC

Understand contributions at higher orders

- The gluon contribution at EIC is small
- Resolved photon contribution

Extract FFs, understand evolution, use heavy mesons in jets

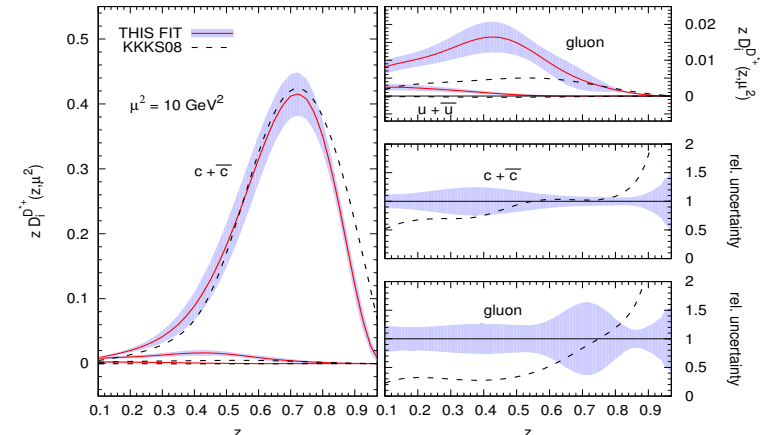
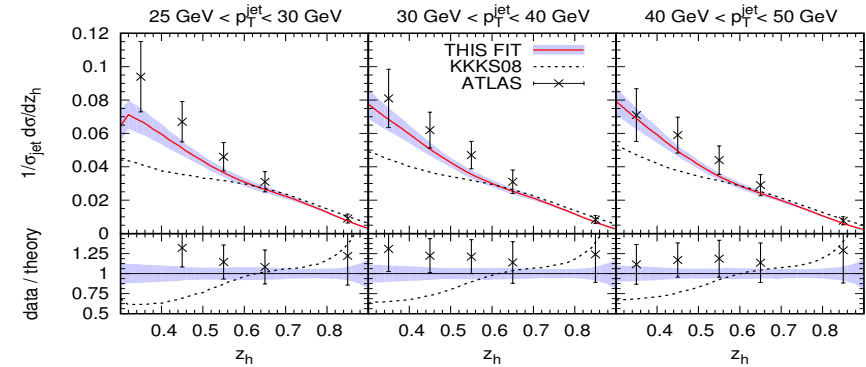
$$\frac{d}{d \ln \mu^2} \tilde{D}^{h/i}(x, \mu) = \sum_j \int_x^1 \frac{dz}{z} \tilde{D}^{h/j}\left(\frac{x}{z}, \mu\right) \times \left( P_{ji}(z, \alpha_s(\mu)) + P_{ji}^{\text{med}}(z, \mu) \right)$$



Braaten *et al.* (1995)

D. Anderle *et al.* (2017)

$$E_h \frac{d^3 \sigma^{\ell N \rightarrow h X}}{d^3 P_h} = \frac{1}{S} \sum_{i,f} \int_0^1 \frac{dx}{x} \int_0^1 \frac{dz}{z^2} f^{i/N}(x, \mu) \times D^{h/f}(z, \mu) \left[ \hat{\sigma}^{i \rightarrow f} + f^{\text{ren}} \left( \frac{-t}{s+u}, \mu \right) \hat{\sigma}^{\gamma i \rightarrow f} \right].$$

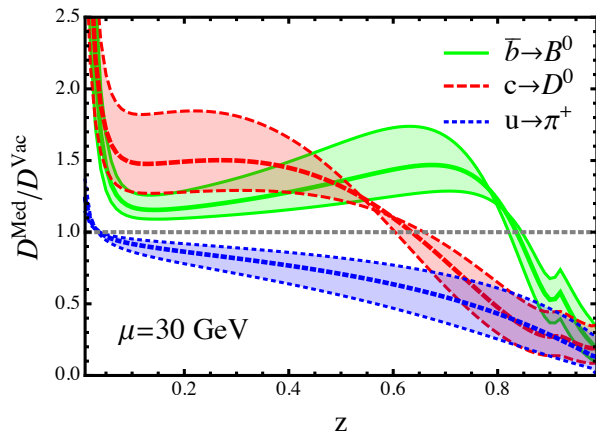




# Modification of FFs in e+A

Vacuum splitting functions provide correction to vacuum showers and correspondingly modification to DGLAP evolution for FFs

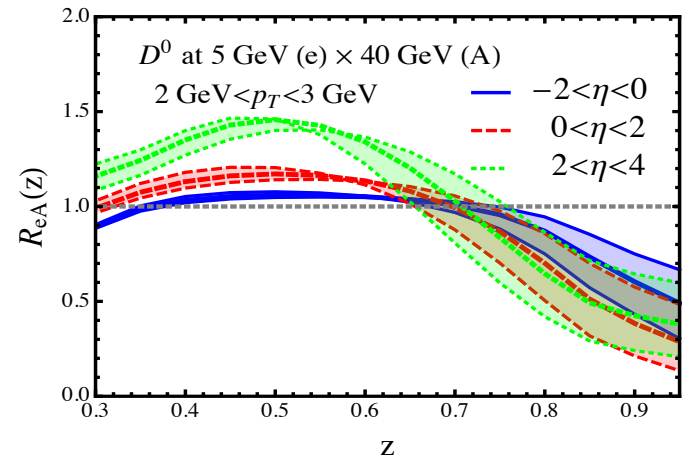
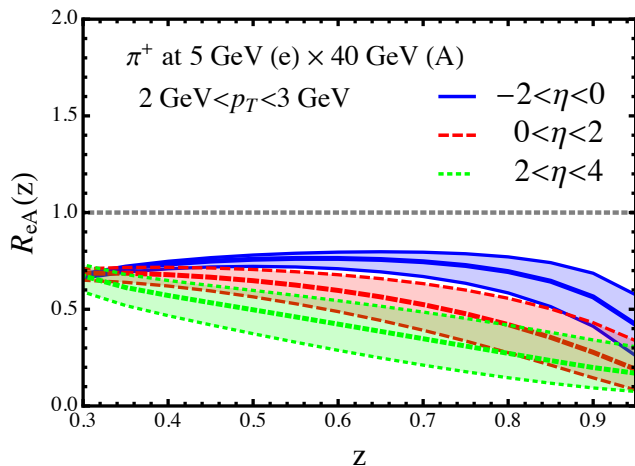
H Li et al. (2020)



$$\frac{dD_q(z, Q)}{d \ln Q} = \frac{\alpha_s(Q^2)}{\pi} \int_z^1 \frac{dz'}{z'} \left\{ P_{q \rightarrow qg}(z', Q) D_q\left(\frac{z}{z'}, Q\right) + P_{q \rightarrow gq}(z', Q) D_g\left(\frac{z}{z'}, Q\right) \right\},$$

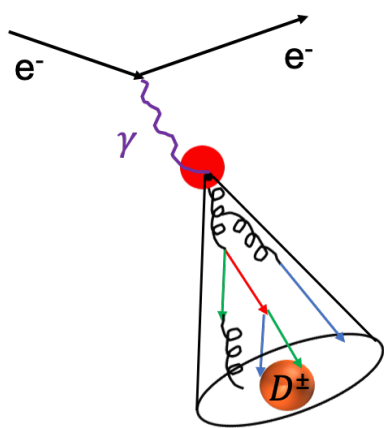
$$\frac{dD_{\bar{q}}(z, Q)}{d \ln Q} = \frac{\alpha_s(Q^2)}{\pi} \int_z^1 \frac{dz'}{z'} \left\{ P_{q \rightarrow qg}(z', Q) D_{\bar{q}}\left(\frac{z}{z'}, Q\right) + P_{q \rightarrow gq}(z', Q) D_g\left(\frac{z}{z'}, Q\right) \right\},$$

$$\frac{dD_g(z, Q)}{d \ln Q} = \frac{\alpha_s(Q^2)}{\pi} \int_z^1 \frac{dz'}{z'} \left\{ P_{g \rightarrow gg}(z', Q) D_g\left(\frac{z}{z'}, Q\right) + P_{g \rightarrow q\bar{q}}(z', Q) \left( D_q\left(\frac{z}{z'}, Q\right) + f_{\bar{q}}\left(\frac{z}{z'}, Q\right) \right) \right\}.$$

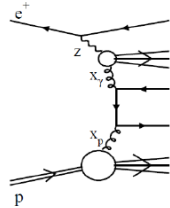


# Jet production at the EIC

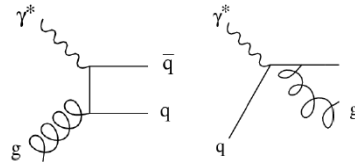
$$e^- + p \rightarrow e^- + jet(D^\pm) + X$$



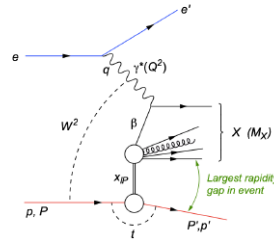
Resolved



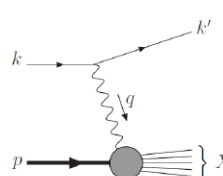
Photon-Gluon Fusion & QCD-Compton



Diffractive

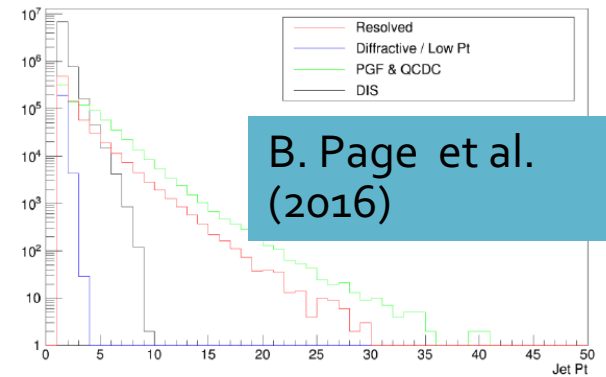


DIS



Large number of contributions to be understood

Inclusive Jet  $p_T$ :  $Q^2 = 10-100 \text{ GeV}^2$



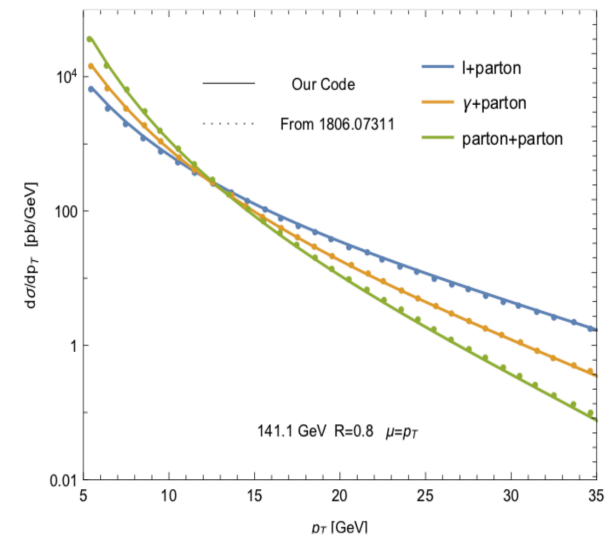
A useful modern way semi-inclusive jet functions – can include  $\ln R$  resummation

$$E_J \frac{d^3 \sigma^{lN \rightarrow jX}}{d^3 P_J} = \frac{1}{S} \sum_{i,f} \int_0^1 \frac{dx}{x} \int_0^1 \frac{dz}{z^2} f_{i/N}(x, \mu) \times \hat{\sigma}^{i \rightarrow f}(s, t, u, \mu) J_f(z, p_T R, \mu),$$

R. Boughezal et al. (2020)

Li et al. (2020)

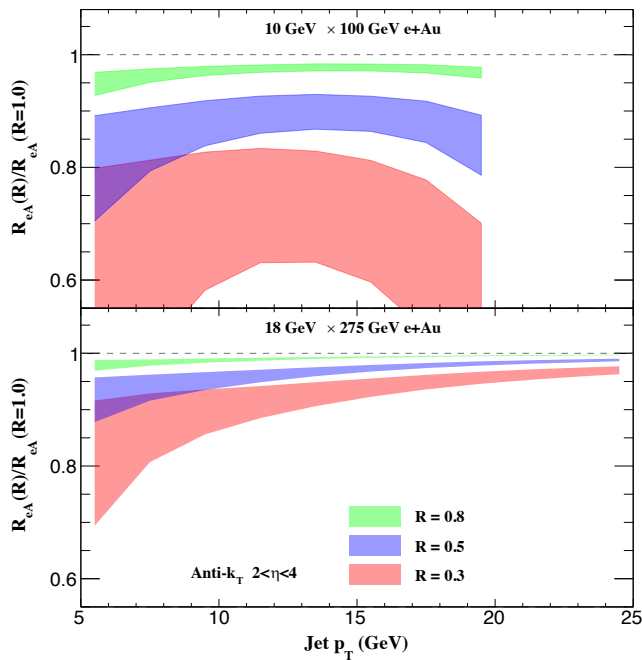
Has to be applied to heavy-flavor tagged jet production at the EIC



# Heavy jet production in e+A

- Modern SCET techniques to calculate heavy jet modification. Applicable to EIC

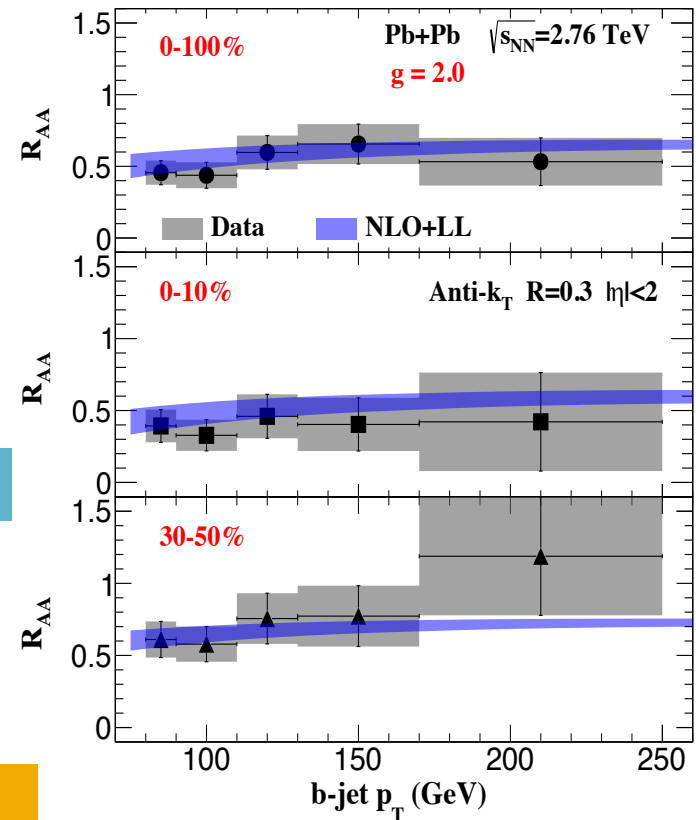
$$J_{J_Q/i}^{\text{med}} = J_{J_Q/i}^{\text{med,(0)}} + \frac{\alpha_s}{2\pi} J_{J_Q/i}^{\text{med,(1)}}$$



H. Li et al. (2020)

H. Li et al. (2018)

## Example from heavy ion collisions

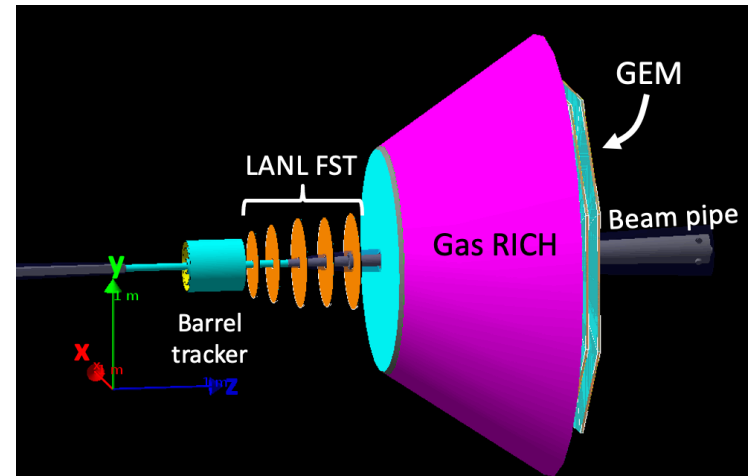
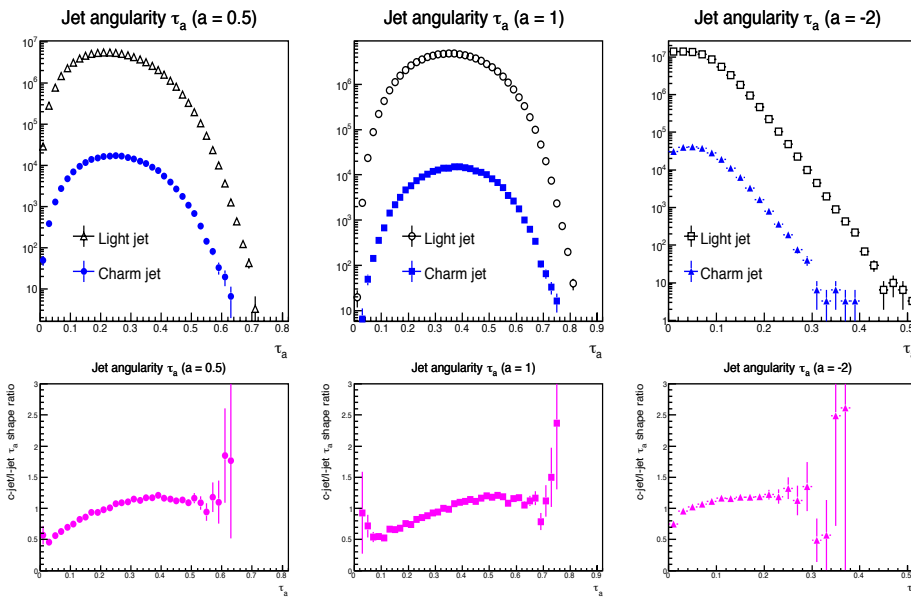


- Understand heavy flavor jet production with nuclei, effect of mass on parton showers

# Heavy flavor jet substructure

Jet substructure (e.g. jet angularity) studies for flavor tagged jets can improve the understanding of flavor dependent hadronization processes.

The asymmetric collisions nature at the EIC requires special focus on the forward going direction

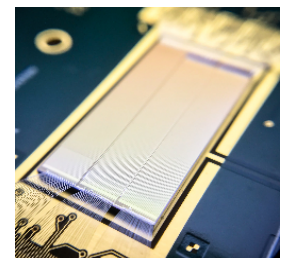
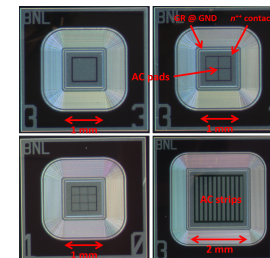
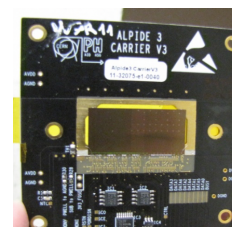


Li et al. arXiv: 2007.14417

MAPS tech.

LGAD tech.

HV-MAPS tech.



Technologies of interest to HEP and NP developed

# Numerical methods

## Refactoring

- Code is **restructured** (in C++) and shortened (**24K** → **8K lines**). **20x speed improvement**

## Effective incorporation of nuclear medium

- **2x speed improvement**

## Efficient on-node parallelization

- New parallelization shows much better scaling **10x speed improvement**

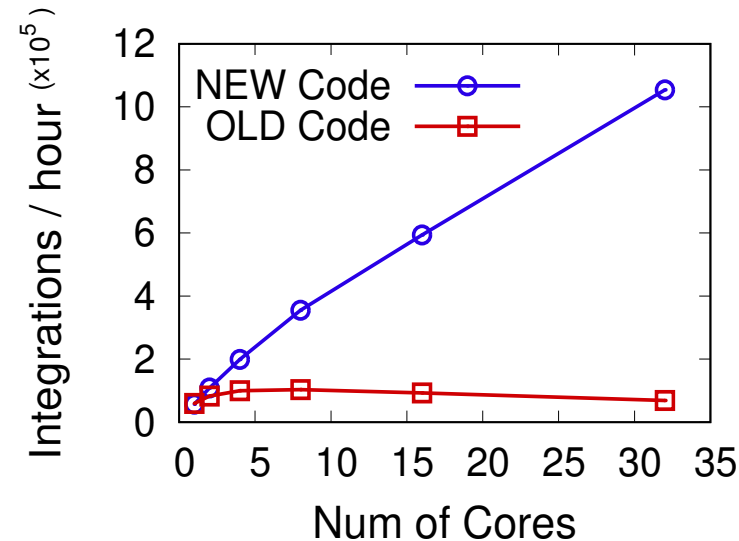
**Overall improvement:**

**18 days** → **1 hour**

**Higher orders till challenging**

- ML techniques investigated

```
if (split_id==1) //Quark-->Quark, Gluon
{
  if (int_id==1)
  {
    Vegas(NDIM, NCOMP, Integrand, gqnocuts, USERDATA,
    EPSREL, EPSABS, verbose, SEED,
    NINEVAL, MAKEVAL, NSTART, NINCREASE, NBATCH,
    GRIDNO, STATEFILE,
    &neval, &fail, integral, error, prob);
  }
  if (int_id==2)
  {
    Suave(NDIM, NCOMP, Integrand, gqnocuts, USERDATA,
    EPSREL, EPSABS, verbose | LAST, SEED,
    NINEVAL, MAKEVAL, NNEW, FLATNESS,
    STATEFILE,
    &neval, &fail, integral, error, prob);
  }
  if (int_id==3)
  {
    Divonne(NDIM, NCOMP, Integrand, gqnocuts, USERDATA,
    EPSREL, EPSABS, verbose, SEED,
    NINEVAL, MAKEVAL, KEY1, KEY2, KEY3, MAXPASS,
    DRIVEN, MAXGRESQ, HIREGISTRATION,
    NGIVEN, LDGIVEN, NULL, NEXTRA, NULL,
    STATEFILE,
    &neval, &fail, integral, error, prob);
  }
  if (int_id==4)
  {
    CuRe(NDIM, NCOMP, Integrand, gqnocuts, USERDATA,
    EPSREL, EPSABS, verbose | LAST,
    NINEVAL, MAKEVAL, KEY,
    STATEFILE,
    &neval, &fail, integral, error, prob);
  }
  if (split_id==2) //Gluon-->Gluon, Gluon
  {
    if (int_id==1)
    {
      Vegas(NDIM, NCOMP, Integrand, gqnocuts, USERDATA,
      EPSREL, EPSABS, verbose, SEED,
      NINEVAL, MAKEVAL, NSTART, NINCREASE, NBATCH,
      GRIDNO, STATEFILE,
      &neval, &fail, integral, error, prob);
    }
    if (cur_id == 1)
    {
      if (cut_id == 1)
      {
        switch(split_id)
        {
          case 1:
            func = &Integrand.gqnocuts; break;
          case 2:
            func = &Integrand.gqnocuts; break;
          case 3:
            func = &Integrand.gqnocuts; break;
          case 4:
            func = &Integrand.gqnocuts; break;
          default:
            print("Error: Unknown split_id %d\n", split_id);
            exit(0);
        }
        // switch(split_id)
      }
      cur_id = 1;
    }
  }
}
```



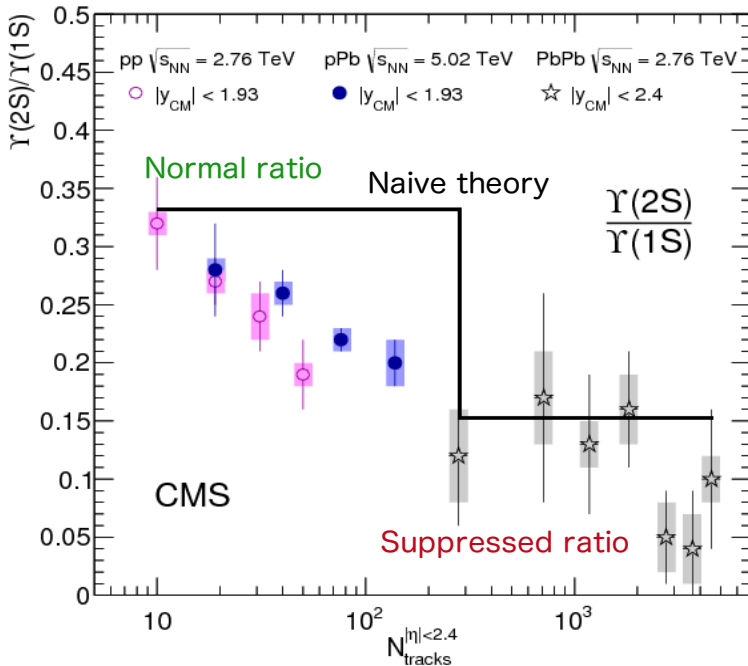
**We have generated grids for medium-induced splitting functions for various nuclei – He, Kr, Xe, Au, Pb**

# Quarkonia production puzzles

- Quarkonia (e.g.  $J/\psi, \Upsilon$ ), bound states of the heaviest elementary particles – still not understood theoretically

Matsui *et al.* (1986)

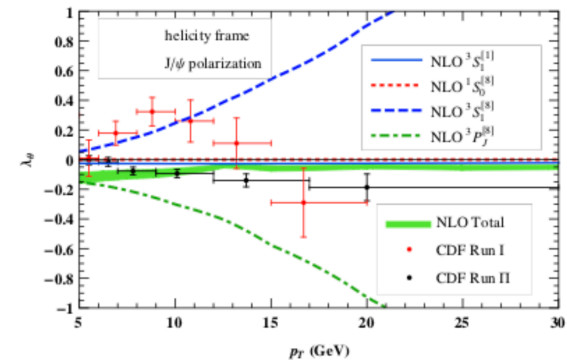
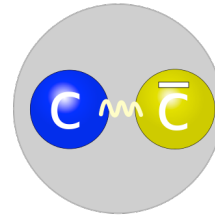
## Excited Upsilon suppression



Chatrachyan *et al.* (2014)

## Outstanding puzzles

- Quarkonium polarization puzzle – inability to simultaneously describe the cross section and polarization of quarkonia

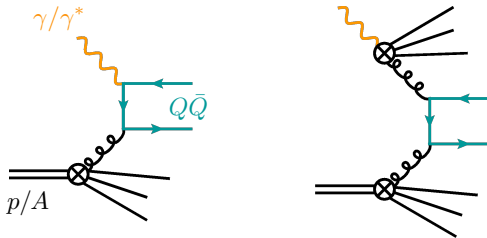


$$\frac{dN}{d \cos \theta} \propto 1 + \lambda_\theta \cos^2 \theta, \quad \lambda_\theta = \frac{d\sigma_{11} - d\sigma_{00}}{d\sigma_{11} + d\sigma_{00}}$$

- Suppression puzzle - similar dissociation behavior observed in small system, p+A and even in p+p (where QGP is not expected), as a function of the number of hadrons.

# Quarkonium production at the EIC

Lepton-nucleon/nucleus collisions constitute an excellent laboratory for the studies of quarkonium production since, it is simplified and cleaner environment compared to hadronic collisions, yet far richer than in the electron-positron annihilation. Quarkonia can be produced either through photo-production ( $Q \sim 0$ ) or lepto-production ( $Q > 1$  GeV) processes. In these two cases the resolved, diffractive/exclusive, and inclusive productions



HERA data has had important impact but interpretation subject of debate

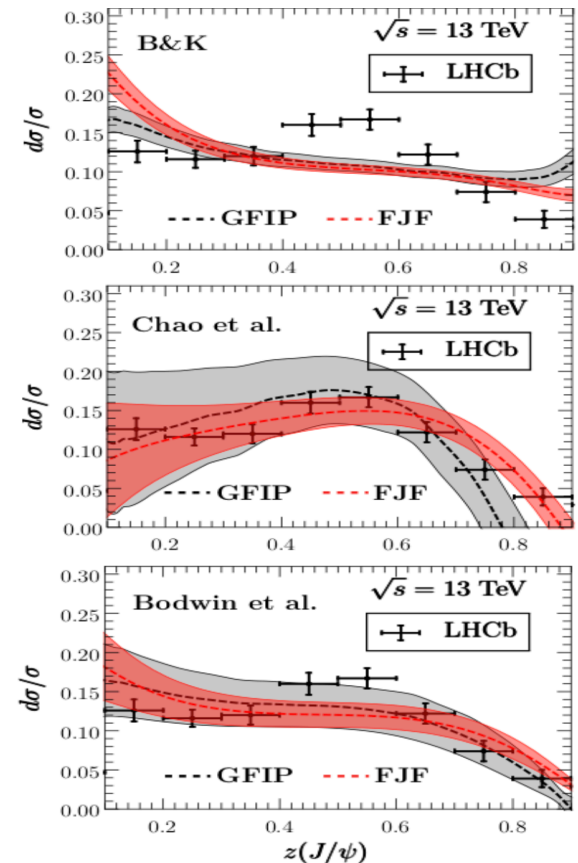
Flore et al. (2020)

There has been no phenomenological extraction of the TMD shape functions. Meanwhile, it has been proposed that exclusive quarkonium production can be understood through the formalism of GPDs and the Wigner functions

Cui et al. (2018)

Chen et al. (2019)

## Constraining matrix elements at EIC



Bain et al. (2017)

# Quarkonium production in reactions with nuclei

## EFTs for quarkonia in matter

- The EIC will also offer the opportunity to observe quarkonium production in eA collisions where one can study the interactions with nuclear matter and the formation of quarkonia in a nuclear medium.

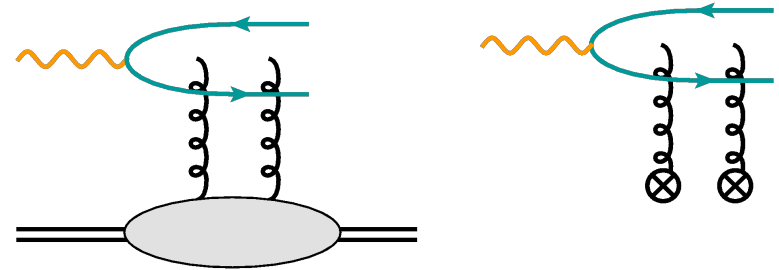
Y. Makris et al. (2019)

## Open quantum systems

- Primarily formulated in the context of quark-gluon-plasma, these formalisms can also be extended to cold nuclear matted effects

Akamatsu et al. (2014)

Yao et al. (2020)



$$\mathcal{L}_{\text{NRQCD}_G} = \mathcal{L}_{\text{NRQCD}} + \mathcal{L}_{Q-G/C}(\psi, A_{G/C}^{\mu,a}) + \mathcal{L}_{g-G/C}(A_s^{\mu,b}, A_{G/C}^{\mu,a}) + \psi \longleftrightarrow \chi$$

## NRQCD with Glauber Gluons

$$\mathcal{L}_{Q-G/C}^{(0)}(\psi, A_{G/C}^{\mu,a}) = \sum_{\mathbf{p}, \mathbf{q}_T} \psi_{\mathbf{p}+\mathbf{q}_T}^\dagger \left( -g A_{G/C}^0 \right) \psi_{\mathbf{p}} \quad (\text{collinear/static/soft}).$$

$$\mathcal{L}_{Q-G/C}^{(1)}(\psi, A_G^{\mu,a}) = g \sum_{\mathbf{p}, \mathbf{q}_T} \psi_{\mathbf{p}+\mathbf{q}_T}^\dagger \left( \frac{2A_G^n(\mathbf{n} \cdot \mathbf{P}) - i[(\mathbf{P}_\perp \times \mathbf{n})A_G^n] \cdot \boldsymbol{\sigma}}{2m} \right) \psi_{\mathbf{p}} \quad (\text{collinear})$$

$$\mathcal{L}_{Q-G/C}^{(1)}(\psi, A_C^{\mu,a}) = g \sum_{\mathbf{p}, \mathbf{q}_T} \psi_{\mathbf{p}+\mathbf{q}_T}^\dagger \left( \frac{2\mathbf{A}_C \cdot \mathbf{P} + [\mathbf{P} \cdot \mathbf{A}_C] - i[\mathbf{P} \times \mathbf{A}_C] \cdot \boldsymbol{\sigma}}{2m} \right) \psi_{\mathbf{p}} \quad (\text{soft})$$